AJNR

Cranial MR Imaging in Neurofibromatosis

James R. Bognanno, Mary K. Edwards, Theodore A. Lee, David W. Dunn, Karen L. Roos and Eugene C. Klatte

This information is current as of August 11, 2025.

Cranial MR Imaging in Neurofibromatosis

James R. Bognanno[1]
Mary K. Edwards[1]
Theodore A. Lee[1]
David W. Dunn[2]
Karen L. Roos[2]
Eugene C. Klatte[1]

Cranial MR images of 53 patients with neurofibromatosis were reviewed to determine the nature, extent, and number of intracranial abnormalities present. All patients studied met tentative definitions established for the diagnosis of neurofibromatosis. Twenty-three were scanned for evaluation of known CNS or cranial nerve involvement; the remainder were neurologically asymptomatic patients without suspected lesions referred for screening. Single lesions were noted in 32 patients. Multiple lesions were identified in 14 patients. Seven had normal scans. In 23 patients small focal areas of increased signal on T2-weighted scans within the brain were thought to represent heterotopias. Eight patients had chiasmal gliomas and two had optic nerve gliomas. Nine patients had parenchymal gliomas, two had ischemic changes, and one had a colloid cyst. Extraaxial lesions included acoustic neuromas (five patients), meningiomas (four), trigeminal neurofibromas (one), and dysplasia of a sphenoid wing (two). Of the 30 asymptomatic patients referred for screening, lesions were found in 23.

MR was found to be an excellent method of imaging known disease and of detecting lesions in asymptomatic patients. Because of the large number of asymptomatic lesions detected in this population, a screening MR study is recommended in patients with neurofibromatosis.

Neurofibromatosis is the most common of the neurocutaneous syndromes. It is estimated to occur in one of every 2000–3000 births [1]. The disorder has been divided into categories with different clinical and pathologic features, including peripheral, central, mixed peripheral, and CNS forms [2–4]. More recently, distinctions have been made between neurofibromatosis I (von Recklinghausen neurofibromatosis), neurofibromatosis II (bilateral acoustic neurofibromatosis), and other forms [5, 6]. Neuroradiology has traditionally played an important role in the evaluation of the myriad CNS manifestations of neurofibromatosis, including cranial nerve schwannomas, meningiomas, pilocytic astrocytomas, gliomas, ependymomas, angiomas, and hamartomatous lesions [1–4, 7].

The plain film and cranial CT findings of neurofibromatosis have been well described [1, 7–10]. The purpose of this investigation was to review the CNS MR findings in patients with neurofibromatosis to help determine the contribution of MR in the diagnosis and evaluation of neurofibromatosis.

Materials and Methods

From 1982 to 1987, 53 patients with neurofibromatosis were referred for cranial MR. All patients studied met the tentative definitions for neurofibromatosis I or II established by the National Institute of Neurological and Communicative Diseases and Stroke and the National Institutes of Health [5, 6]. A review of the medical records revealed that 23 patients had clinical or prior CT findings consistent with intracranial or cranial nerve abnormalities. Thirty patients referred for screening evaluation as a part of this study were asymptomatic neurologically without suspected CNS disease. The patients were 2–70 years old (mean, 18 years).

In 40 of the 53 patients recent cranial CT scans were available for comparison. MR images

were obtained in 26 patients with a resistive magnet* operating at 0.15 T and in 15 patients with an MR superconducting magnet[†] operating at 1.5 T. Twelve patients were scanned on both units. Images were obtained by using spin-echo pulse sequences with T1-weighting (550/32 [TR/TE]) and T2-weighting (2000/120) on the 0.15-T magnet. Two patient were studied with inversion-recovery techniques no longer performed at this institution. Scans obtained on the 1.5-T magnet used spin-echo and multiecho pulse sequences. A variety of T1-weighted sequences were used, predominantly 700/30. Proton-density- and T2-weighting sequences used primarily 2000/20–90. All images were obtained in the axial plane and supplemented as necessary with sagittal and/or coronal sections.

Results

In 46 of the 53 patients studied by MR, parenchymal CNS or extraaxial intracranial lesions were seen. Single types of lesions were identified in 32 patients and multiple types in 14 (Table 1). The types of lesions included small focal areas of increased T2 signal postulated to represent heterotopia, optic nerve and chiasmal gliomas, parenchymal gliomas, ischemic changes, and a colloid cyst. Extraaxial lesions such as acoustic neuromas, meningiomas, trigeminal neurofibromas, and dysplasia of a sphenoid wing were also observed.

Heterotopia

Small focal areas of increased signal within the brain parenchyma on T2-weighted images were identified in 23 patients: 16 asymptomatic screening patients and seven patients studied for other known lesions or symptoms. Although the exact nature of these lesions is unclear, we postulate that they represent focal areas of heterotopic or possibly dysplastic tissue. They were located primarily in the basal ganglia and internal capsule with other lesions seen in the midbrain, cerebellum, and subcortical white matter. CT and T1-weighted MR images revealed few or no abnormalities in corresponding locations (Figs. 1 and 2). Other CNS abnormalities were seen in 10 of these patients, including five optic nerve or chiasmal gliomas, one with multiple gliomas, one with a brainstem glioma, one with a low-grade cerebral glioma, one with a midbrain lesion presumed to represent a low-grade glioma, and one with acoustic neuromas and multiple meningiomas. Thirteen patients had hamartomatous lesions only without other abnormalities. All 13 were part of the screening population with no acute symptoms, although two had developmental delay and two had long-standing seizure disorders. Follow-up scans have been obtained in six of the 23 patients; in two of these, lesions were seen on high-field scans that were not seen on prior low-field scans, three showed no apparent change from low- to high-field follow-up scans or on subsequent high-field follow-up scans, and one appeared to develop new similar lesions (Fig. 3).

Optic Nerve and Chiasmal Gliomas

One patient with a known optic nerve glioma was studied with MR. There was enlargement of the affected optic nerve

---

* Teslacon, Technicare.
[†] Vista, Picker.

TABLE 1: MR Findings in Asymptomatic and Symptomatic Neurofibromatosis Patients with Single and Multiple Types of Lesions

Type of Lesions: MR Diagnosis	No. of Patients	
	Asympto-matic	Sympto-matic
Single:		
Normal	7	0
Heterotopia	13	0
Chiasmal glioma	2	2
Parenchymal glioma	0	3
Acoustic neuroma	0	2
Trigeminal neuroma	0	1
Ischemic changes	2	0
Hydrocephalus	0	2
Sphenoid wing dysplasia	0	2
Chiari I malformation	2	0
Colloid cyst	1	0
Multiple:		
Optic nerve or chiasmal glioma and heterotopia	3	2
Chiasmal glioma and hydrocephalus	0	1
Parenchymal glioma and heterotopia	0	3
Brainstem glioma, hydrocephalus, and heterotopia	0	1
Cervical cord astrocytoma and meningioma	0	1
Brainstem glioma, acoustic neuroma, and meningioma	0	1
Acoustic neuroma and meningioma	0	1
Acoustic neuroma, meningioma, and heterotopia	0	1
Total	30	23

with no abnormal signal intensity on T2-weighted images. A second patient studied as part of the screening population was noted to have enlargement of the optic nerves and chiasm, also without signal abnormality. Heterotopias in the region of the basal ganglia were found in both these patients.

Eight patients with chiasmal gliomas were evaluated with MR. Four were discovered as part of the screening population, three had known lesions, and one was being evaluated for precocious puberty. Of these, 1 had hydrocephalus and four had heterotopias (Fig. 4). The patient with hydrocephalus had prior radiation therapy, and no MR abnormalities were seen in the optic tracts. In seven, presumed extension along the optic tracts was identified with MR (Fig. 5). In two of the seven this finding was noted on CT as contrast enhancement in the optic tracts. Increased signal on T2-weighted images was consistently present in the primary glioma and in areas of gliomatous extension. Anatomic changes were observed on T1-weighted images in the primary glioma and surrounding brain secondary to mass effect, while little or no mass effect was seen in the areas of gliomatous extension.

Parenchymal Gliomas

Nine patients with parenchymal gliomas were studied with MR. Eight had known lesions and one was being evaluated
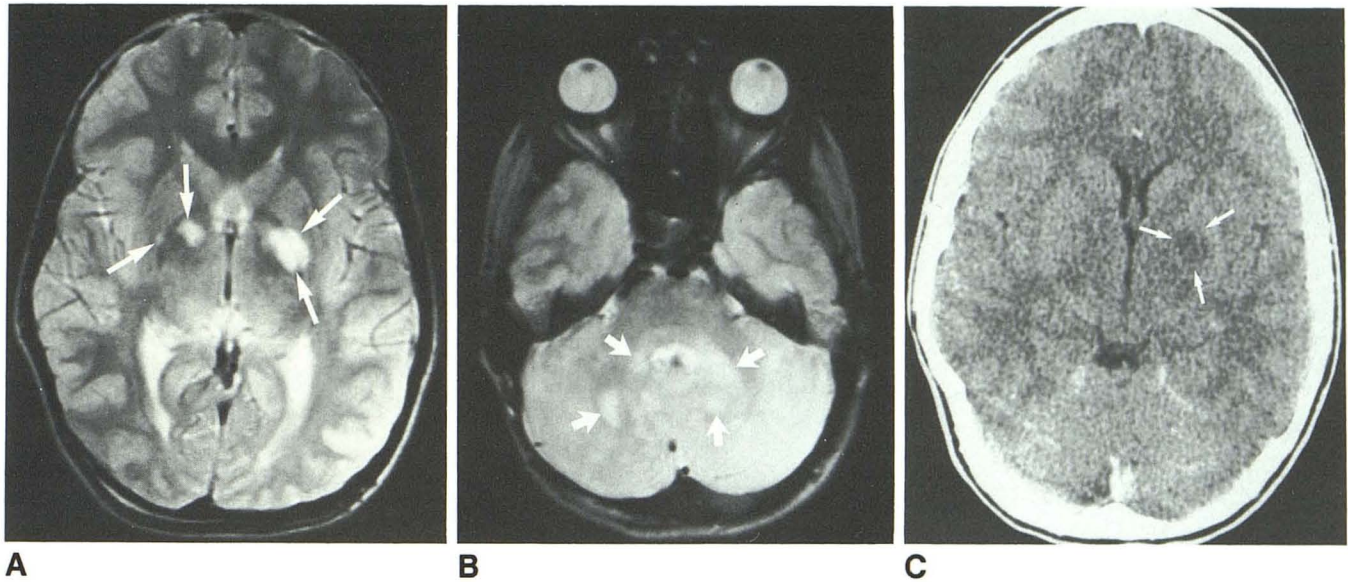
Fig. 1.—Asymptomatic 10-year-old boy.
A, High-field MR image, 2000/90. Bilateral heterotopia (*arrows*) in region of basal ganglia and internal capsule.
B, High-field MR image, 2000/90, through cerebellum shows similar lesions (*arrows*).
C, Contrast-enhanced CT scan. Area of slightly decreased attenuation (*arrows*) corresponds to lesion seen on MR.
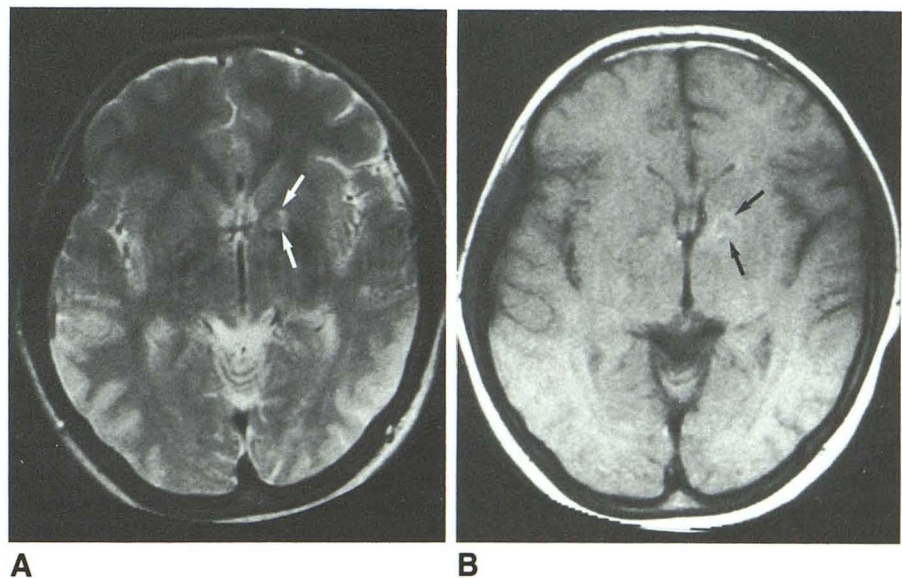

Fig. 2.—High-field MR images in asymptomatic 15-year-old girl.
A, T2-weighted image, 2000/90. Left basal ganglia heterotopia (*arrows*).
B, T1-weighted image, 700/30. Slightly increased signal in region of heterotopia (*arrow*), presumably from strong T2 effect.

for a new hemisensory deficit. The lesions included one cystic parietal glioma (Fig. 6), two multicentric gliomas (Fig. 7), one low-grade calcified parietal glioma, one midbrain lesion postulated to represent a low-grade glioma, two brainstem gliomas, one cystic cerebellar astrocytoma, and one cervical cord astrocytoma with a syrinx. Four of these patients also had heterotopias, one had meningiomas, and one had acoustic neuromas and meningiomas. MR features of parenchymal gliomas included homogeneous increased signal in tumor cysts and slightly inhomogeneous increased signal from the solid tumors. Decreased signal on T1-weighted images was

occasionally noted in the tumor nidus. Varying degrees of white-matter edema surrounding the tumors were noted. Mass effect was noted in all cases. Obstructive hydrocephalus was seen in only one case. Sagittal images were most helpful in defining the extent of tumor in the two cases of brainstem glioma and in the one case of cervical cord glioma.

In one case, a patient with a grade-II astrocytoma of the right parietal lobe was noted on preoperative MR to have a second mass in the splenium of the corpus callosum with increased signal and a cerebellar mass with heterogeneous signal isointense relative to brain on a T2-weighted sequence
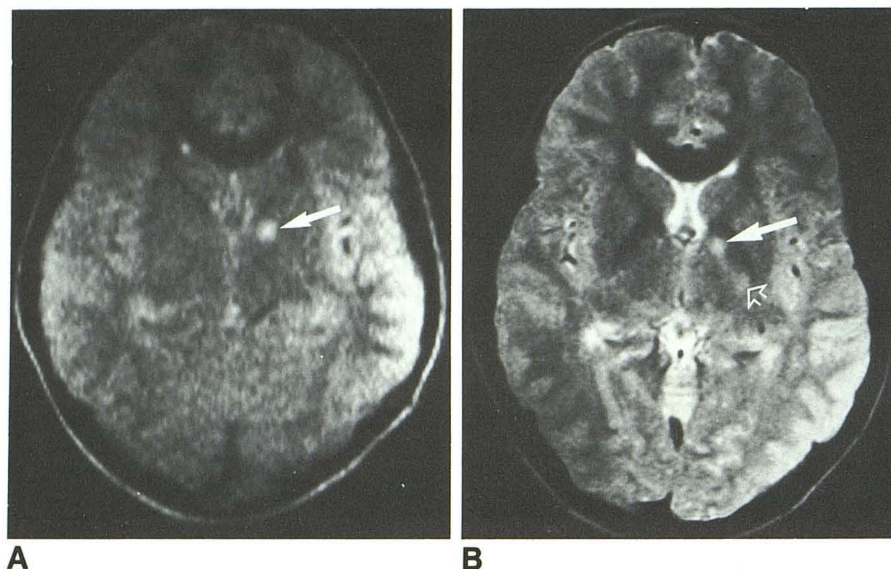
A   B

Fig. 3.—15-year-old girl with known optic nerve glioma.
A, Low-field MR image, 2000/120. Small area of increased signal near genu of left internal capsule (*arrow*) was thought to be a heterotopia.
B, High-field MR image, 2000/90, 2 years later. No change in original lesion (*solid arrow*). Probable new lesion in posterior limb of left internal capsule (*open arrow*).
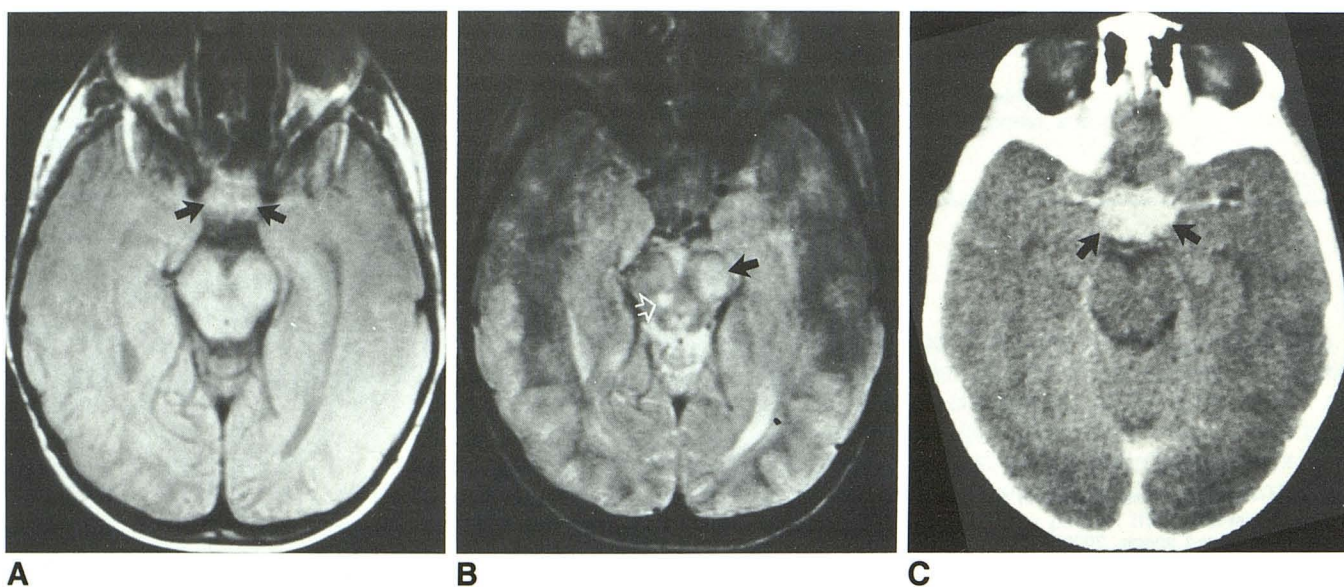

A   B   C

Fig. 4.—Asymptomatic 9-year-old boy referred for screening.
A, High-field proton-density image, 2000/20. Chiasmal glioma (*arrows*).
B, High-field T2-weighted image, 2000/90. Left cerebral peduncle lesion (*solid arrow*) and smaller right tegmentum lesion (*open arrow*) are thought to represent heterotopias.
C, Contrast-enhanced CT scan. Densely enhancing chiasmal glioma (*arrows*). No abnormalities identified in midbrain.

(Fig. 7). The signal characteristics of the splenium and cerebellar masses did not change after surgery or radiation therapy. No calcification was present in the cerebellar mass on CT. The cerebellar mass was presumed to represent a low-grade tumor, although no biopsy was performed.

Acoustic Neuromas and Meningiomas

Five patients with acoustic neuromas were examined with MR. All were symptomatic. The neuromas appeared as mass lesions in the cerebellopontine angles with isointense or sometimes increased or mixed signal on T2-weighted images. Coronal imaging with thin sections (3 mm) was useful in delineating the extent of the lesions. Two patients had acoustic neuromas only. Three had multiple meningiomas (Fig. 8), one of whom also had hamartomatous lesions and one a brainstem glioma. Four patients with meningiomas were studied, three of whom are described above. One other patient had multiple meningiomas and a cervical cord astrocytoma.

Fig. 5.—Asymptomatic 9-year-old boy.

A, High-field MR image, 2000/90. Increased signal from chiasm (*solid arrows*) and adjacent optic tracts (*open arrows*).

B, Same scan (2000/90), contiguous cut. Increased T2 signal in optic tracts (*arrows*), right greater than left, was presumed to represent gliomatous spread. Small midbrain lesions were presumed to represent heterotopias.

C, Contrast-enhanced CT scan with enhancement in region of optic chiasm and hypothalamus (*arrows*).
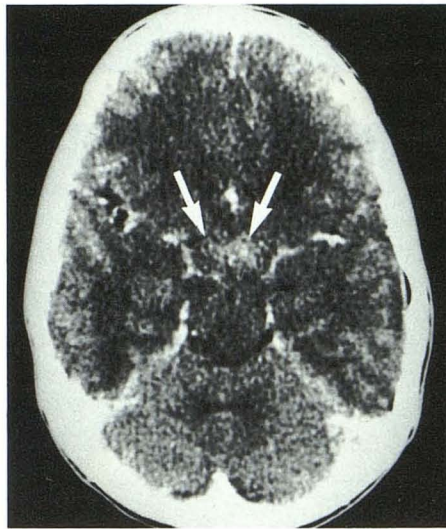
D, At level similar to *B*. No abnormality is identified.

A
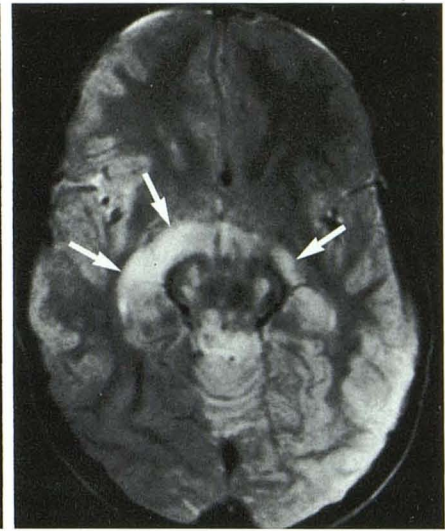
B

C

D

Ischemic Changes

Two patients over age 55 had ischemic changes. In both, periventricular white-matter ischemic changes were manifested by increased signal on T2-weighted images. Lacunar infarcts were also identified in these patients as discrete areas of more intense signal on T2-weighted images and corresponding focal areas of decreased signal on T1-weighted scans. These lesions were confirmed by CT findings characteristic of lacunar infarcts.

Other

Two patients had hydrocephalus without other abnormality on MR or CT. In two patients a Chiari I malformation was seen on MR, although CT and other MR findings were normal. One patient was studied with large neurofibromas of the trigeminal nerves arising from the gasserian ganglia (Fig. 9). In two patients dysplasia of a sphenoid wing was observed. One asymptomatic patient was discovered to have a small round lesion within the third ventricle with increased signal on

Fig. 6.—16-year-old boy with biopsy-proved left parietal glioma. Low-field MR image, 2000/120, shows glioma and/or edema (*arrow*) and intense signal from cystic component (*arrowheads*).
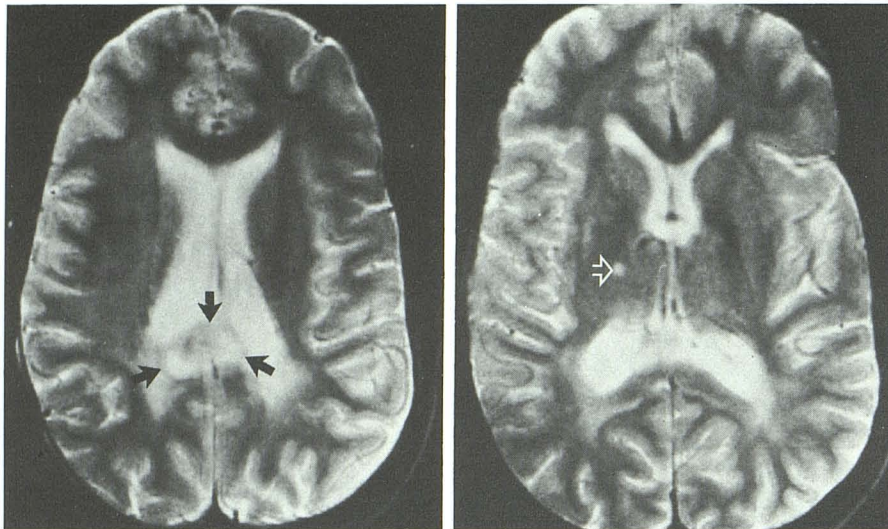
A

B
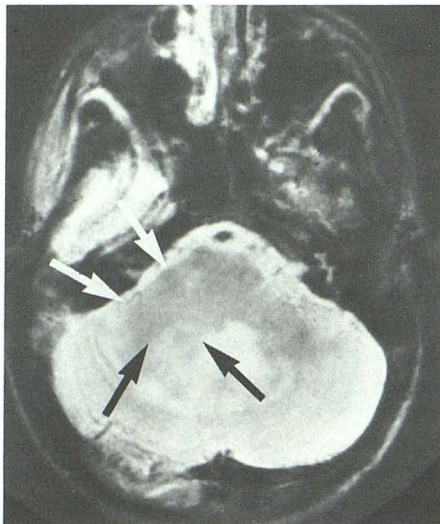
C
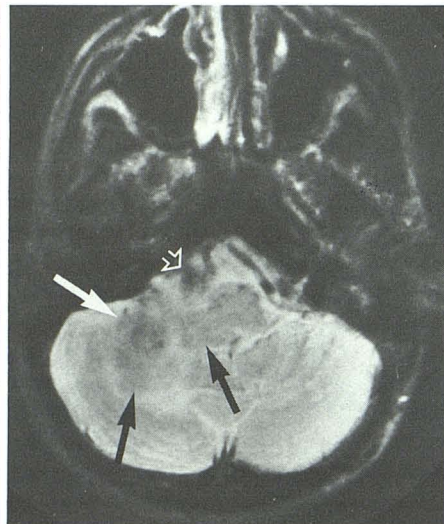
D

Fig. 7.—16-year-old boy with presumed multicentric gliomas after subtotal resection of a grade-II right parietal astrocytoma and 5000 rad (50 Gy) of whole-brain irradiation. High-field MR images, 2000/90.

A, Synchronous mass of splenium of corpus callosum (*arrows*) was presumed to be second glioma.

B, Punctate lesion in right basal ganglia (*arrow*) was considered to represent a heterotopia.

C, Mass involving right cerebellar hemisphere, brachium points, and pons (*arrows*). Mass has heterogeneous, isointense signal. Surrounding increased signal from white matter of cerebellum was presumed to represent edema.

D, Adjacent inferior cut. Mass and presumed edema (*solid arrows*) with exophytic component near right vertebral artery and brainstem (*open arrow*).
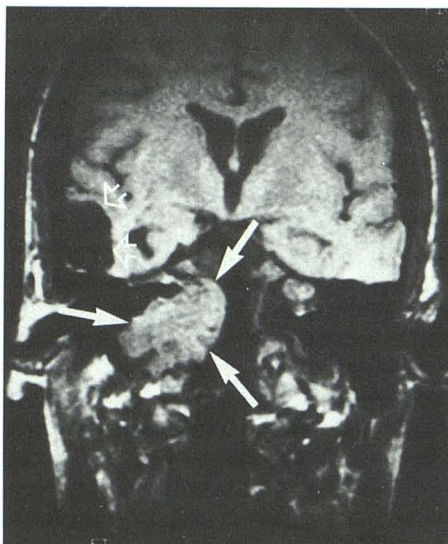
A
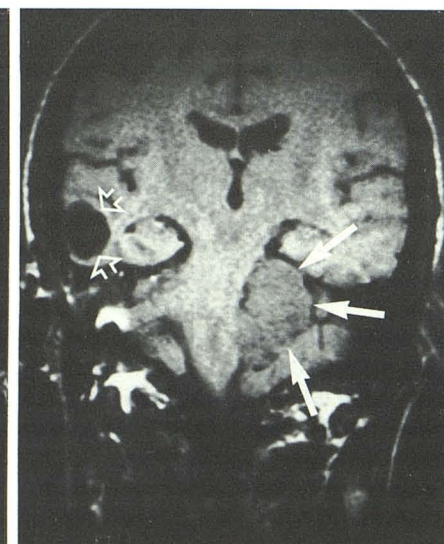
B

Fig. 8.—36-year-old man with bilateral acoustic neuromas and multiple meningiomas. High-field MR images, 833/26.

A, Acoustic neuroma in right cerebellopontine angle (*solid arrows*). Right temporal meningioma (*open arrows*).

B, Acoustic neuroma in left cerebellopontine angle (*solid arrows*) with brainstem displacement to right. Same right temporal meningioma (*open arrows*).
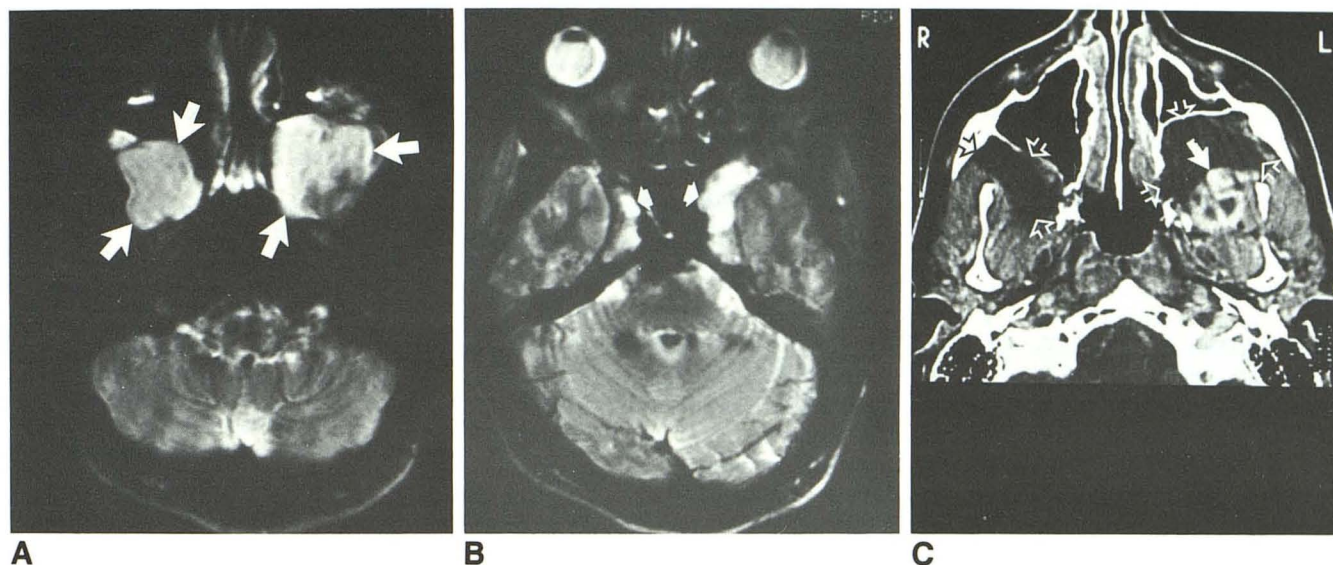
Fig. 9.—26-year-old man with bilateral facial masses, blurred vision, and headaches.
A, High-field MR image, 2000/90, shows bilateral neurofibromas of trigeminal nerves within infratemporal fossae (*arrows*).
B, High-field MR image, 2000/90, shows intracranial component of tumors within cavernous sinuses bilaterally (*arrows*).
C, Contrast-enhanced CT scan. Left infratemporal fossa neurofibroma with vascular enhancement (*solid arrow*). Low-density neurofibromas (*open arrows*).

T1- and T2-weighted scans compatible with a colloid cyst. Subsequent CT findings were characteristic of this type of lesion. Seven patients had normal MR examinations. CT scans were normal in four of the seven; in the other three no CT scans were available for comparison.

Discussion

Our review of 53 patients followed in the Indiana University Neurofibromatosis Clinics included 23 patients with known CNS or cranial nerve lesions and 30 asymptomatic patients referred for screening. Of the asymptomatic patients referred for screening, CNS lesions were found in 23. In this series the high incidence of intracranial abnormalities in asymptomatic patients appear to be important and probably justifies at least one baseline MR examination in this population.

The exact nature of the small parenchymal lesions found in 23 patients is not clear. No histologic confirmation is available in our series. However, because of the appearance and location, these lesions are postulated to represent small areas of heterotopic or dysplastic tissue. The pathologic varieties of heterotopias in neurofibromatosis include meningioangiomatous malformations, atypical glial cell nests, subependymal glial nodules, ependymal ectopias, and intramedullary schwannosis. These are reported to be located primarily in the cerebral cortex and occasionally in the basal ganglia, hypothalamus, cerebral peduncles, and spinal cord [1, 2, 4, 11]. The interest in these lesions lies in their frequency and topographic location, since they are found proximal to clearly neoplastic lesions on pathologic examination [12]. Many authors have postulated them to be a source of some intracranial neoplasms in neurofibromatosis [2, 12–16]. The MR appear-

ance of increased T2 signal from these lesions suggests increased free water content. Whether this is interstitial owing to incompetence of the blood-brain barrier in these lesions or intracellular owing to an abnormality of cellular physiology is uncertain. Radiologic-pathologic correlation will be necessary to determine the significance on this finding.

These small parenchymal lesions were seen in 16 asymptomatic patients referred for screening. Two patients were also discovered to have chiasmal gliomas, one with enlargement of the optic nerves and chiasm. All of these patients will continue to be followed for any changes.

Optic chiasm gliomas are reported to be the most common glioma in neurofibromatosis, falling into the category of pilocytic astrocytomas [7, 17–20]. The incidence in patients with neurofibromatosis has been reported to range from 15–35% [1, 7, 21, 22]. Although CT detected the optic nerve and chiasmal gliomas in each case, MR was more sensitive in defining what appears to be optic-tract extension and improved anatomic definition by using multiple imaging planes. Four chiasmal gliomas were discovered as part of the screening population of this study. All demonstrated extension along the optic tracts. In one patient with enlargement of the optic nerves and chiasm, no abnormality referable to the optic tracts was found. In one series two-thirds of optic nerve or chiasm gliomas in neurofibromatosis patients were asymptomatic and not evident on physical examination at the time of diagnosis [22].

The increased incidence of gliomatous tumors in neurofibromatosis has been well documented [3, 7, 17, 23]. MR accurately defined the extent of tumor involvement in each of the nine cases of parenchymal gliomas in our series. Multiplanar imaging often provided additional information about tumor extension. In one case the CT diagnosis of suspected

venous angioma in a patient with a new hemisensory deficit was changed to that of probable low-grade glioma. This was based on the MR findings of mass effect and surrounding abnormal T2 signal. No biopsy was performed. The significance of the signal characteristics of the cerebellar mass identified in the patient with astrocytomas is uncertain. All of the meningiomas and acoustic neuromas in our series were identified on MR images. In some of these cases the MR examination added to the evaluation with coronal imaging and improved imaging of the posterior fossa.

The results of our review corroborate a number of concepts about the CNS findings in neurofibromatosis: (1) the manifestations are often multifocal [1, 7, 11, 17], (2) a significant number of patients have clinically silent lesions [3, 7, 11, 17], and (3) these patients have an increased propensity for malignant changes [3, 4, 17]. MR was extremely useful in diagnosing and defining the extent of the many intracranial manifestations in neurofibromatosis. We believe that high-field MR is even more sensitive in identifying these abnormalities.

In summary, we found MR to be an excellent method of imaging the many varied and potentially confusing manifestations of neurofibromatosis. MR revealed a significant number of clinically silent lesions. The high incidence of intracranial lesions in these patients probably warrants a baseline cranial MR study in this population.

REFERENCES

1. Gardeur D, Palmieri A, Mashaly R. Cranial computed tomography in the phakomatoses. *Neuroradiology* **1983**;25:293–304
2. Rubenstein LJ. Tumors and tumor-like lesions of maldevelopmental origin. In: Firminger HI, ed. *Tumors of the central nervous system.* Washington, DC: Armed Forces Institute of Pathology, **1972**:285–332
3. Pearce J. The central nervous system pathology in multiple neurofibromatosis. *Neurology* **1967**;17:691–697
4. Lott IT, Richardson EP, Jr. Neuropathological findings and the biology of neurofibromatosis. *Adv Neurol* **1981**;29:23–32
5. Mulvihill JJ, ed. Tentative definitions of neurofibromatosis. *Neurofibroma-*
tosis Res Newsletter **1986**;2(2):1
6. Riccardi VM. Alternative forms of neurofibromatosis. In: *Neurofibromatosis: program and abstracts. NIH Consensus Development Conference,* July **1987**:32–35
7. Jacoby CG, Go RT, Beren RA. Cranial CT of neurofibromatosis. *AJR* **1980**;135:553–557
8. Klatte EG, Franken EA, Smith JA. The radiographic spectrum in neurofibromatosis. *Semin Roentgenol* **1976**;11:17–33
9. Maki Y, Enomoto T, Nose T, et al. Computed tomography in von Recklinghausen's disease. *Childs Nerv Syst* **1980**;8:452–460
10. Salbolino U, Pasquini U, Babin E, Gasquez P. von Recklinghausen's disease and computed tomography. *J Belge Radiol* **1978**;61:313–318
11. Rosman NP, Pearce J. The brain in multiple neurofibromatosis. A suggested neuropathological basis for the associated mental defect. *Brain* **1967**;90:829–838
12. Rubinstein LJ. The malformative central nervous system lesions in the central and peripheral forms of neurofibromatosis. A neuropathological study of 22 cases. *Ann NY Acad Sci* **1986**;486:14–29
13. Taylor PE. Encapsulated glioma of the sylvian fissure associated with neurofibromatosis. Report of a case with histopathological comparison of surgical lesion and autopsy specimen following recurrence. *J Neuropathol Exp Neurol* **1982**;21:566–578
14. Nevin S. Gliomatosis cerebri. *Brain* **1938**;61:170–197
15. Scharinberg K, Jones E. Diffuse glioma of the brain in von Recklinghausen's disease. *Neurology* **1956**;6:269–274
16. Epstein NE, Rosenthal AD, Selman J, et al. Moderate grade astrocytoma presenting in a 4-month old child with a family history of von Recklinghausen's neurofibromatosis spanning four generations: a case report. *Neurosurgery* **1983**;13:692–695
17. Canale D, Bebin J, Knighton RS. Neurologic manifestations of von Recklinghausen's disease of the nervous system. *Appl Neurophysiol* **1964**;24:359–403
18. Holt JF. Neurofibromatosis in children. *AJR* **1978**;130:615–639
19. Kingsley DPE. CAT in the phakomatoses. In: du Boulay GH, Mosley I, eds. *The first European seminar on computerized axial tomography in clinical practice.* Berlin:Springer, **1977**:174–180
20. Riccardi VM, Mulvihill JJ, eds. Neurofibromatosis (von Recklinghausen's disease). *Adv Neurol* **1981**;29:1–282
21. Bailey RO, Herman JD. The role of the cells of Schwann in the formation of tumors of the peripheral nerves. *Am J Pathol* **1938**;14:1–36
22. Lewis RA, Gerson LP, Axelson KA, et al. von Recklinghausen's neurofibromatosis. II. Incidence of optic gliomata. *Ophthalmology* **1984**;91:929–935
23. Rodrigues HA, Berthong M. Multiple primary intracranial tumors in von Recklinghausen's neurofibromatosis. *Arch Neurol* **1966**;14:467–475